ISSN 1075-7015, Geology of Ore Deposits, 2022, Vol. 64, No. 5, pp. 300–312. © The Author(s), 2022. This article is an open access publication, corrected publication 2022.
Russian Text © The Author(s), 2022, published in Geologiya Rudnykh Mestorozhdenii, 2022, Vol. 64, No. 5, pp. 471–484.

# Rare Earth–Uranium–Thorium Mineralization in the Molybdenum Ores of the Buluktaevskoe Mo–W Deposit (Western Transbaikalia, Russia)

**B. B. Damdinov[a], *, L. B. Damdinova[a], and S. Z. Tugutova[a]**

[a] *Dobretsov Geological Institute, Siberian Branch, Russian Academy of Sciences, Ulan-Ude, 670047 Russia*

**e-mail: damdinov@mail.ru*

Received August 3, 2021; revised October 15, 2021; accepted October 15, 2021

**Abstract**—The Buluktaevskoe molybdenum–tungsten deposit is considered a close analog of W–Mo deposits within the large Dzhida orefield, in which the Pervomaiskoe molybdenum and Inkurskoe and Kholtosonskoe tungsten deposits are known. Fifteen ore minerals were identified in the molybdenum ores of the Buluktaevskoe deposit; in addition to molybdenite, they include sulfides (pyrite, galena, and chalcopyrite), tungstates (wolframite and scheelite), molybdates (powellite and wulfenite), and a relatively large number of minerals containing rare earth elements (REE), U, and Th (Th-bearing monazite, brannerite, thorite, and uraninite); among them are previously unknown minerals: fluorine-bearing thorium molybdate and minerals with compositions corresponding to rare mineral species, orthobrannerite and kobeite-(Y). Interrelations and specific chemical compositions of the uranium–thorium–rare earth element minerals are discussed. It was established that these minerals formed in the course of hydrothermal alteration processes, at the early (molybdenite) development stage of the Buluktaevskoe molybdenum–tungsten deposit.

**Keywords:** Buluktaevskoe Mo–W deposit, mineralogy, uranium–thorium–REE minerals

**DOI:** 10.1134/S1075701522050026

## INTRODUCTION

The Buluktaevskoe Mo–W deposit is located in the southwestern part of Western Transbaikalia, almost on the Russian–Mongolian border, in the Zakamensk district of the Republic of Buryatia, 75 km east of the town of Zakamensk, the regional center (285 km southwest of the city of Ulan-Ude). The deposit was discovered in 1933 and was mined from 1938 to 1942. At the beginning, a prospecting team organized tungsten concentrate production, and molybdenum production was carried out since 1941 by the Dzhida mining and concentration complex. The remaining resources of the deposit in the amount of 9.2 thousand tons $WO_3$ and 1.48 thousand tons of molybdenum were written off from the balance sheet by the State Committee for Mineral Reserves in 1990 (Gordienko et al., 2018). However, in spite of the long exploration history of this deposit, many questions concerning the composition and genesis of the molybdenum–tungsten mineralization remain unresolved. Among them is the presence of REE–U–Th mineralization, which was mentioned earlier in the ores of some Mo–W greisen deposits (e.g., Rekharskii, 1973; Kiseleva et al., 1994). The studies of such mineralization are of special interest due to the growing demand for the ores of high-tech metals (Bortnikov et al., 2016).

The Buluktaevskoe molybdenum–tungsten deposit is considered as a close analog of the W–Mo deposits within the large Dzhida orefield (Pervomaiskoe molybdenum deposit; Inkurskoe and Kholtosonskoe tungsten deposits). For instance, the Buluktaevskoe deposit, as well as the others in the Dzhida orefield, is characterized by multistage ore formation process with the early molybdenum association succeeded by the later tungsten association, vein–stockwork morphology of orebodies, and wallrock greisenization. At the same time, distinguishing features are also present: (1) the co-occurrence of the ore with polymictic breccia; (2) the older age of the deposit. In addition, our studies of the molybdenum ores of the Buluktaevskoe deposit demonstrated a number of differences in mineral composition. First of all, this is the presence in the ores of the Buluktaevskoe deposit of U–Th–REE-bearing minerals, which are comparatively scarce in the vein–stockwork W–Mo greisen deposits (Rundkvist et al., 1971). The presence of several thorium–uranium–rare earth mineral varieties in the ores of the Buluktaevskoe deposit raises the question of their origin and the nature of relationship between the uranium–thorium mineralization and the main economic ores. In addition, rare and unnamed U–Th–REE-bearing minerals have been identified in

the ores, and their detailed descriptions will enable us to determine their species.

## GEOLOGICAL OVERVIEW

*Buluktai–Kharatsai ore cluster.* The Buluktaevskoe deposit is located within the Buluktai–Kharatsai ore cluster of the Dzhida ore district in the southwestern part of the Sayan–Baikal foldbelt (Gordienko et al., 2018). The ore cluster is located at the eastern termination of the Dzhida ore district and partially extends into the territory of Mongolia. The area of the ore cluster is composed mainly by intrusive rocks of various compositions; outcrops of the essentially sedimentary limestone–sandstone–shale strata of the Dzhida Formation were established only in its western part, and sporadic fragments of the basalt–andesitic and trachytic volcanics of the Petropavlovsk Formation, in the eastern *(*Fig. 1). The bulk of intrusive rocks are the Middle Permian granitoids of the Dzhida Complex and the small bodies and dikes of the granites and leucogranites of the Gudzhir complex. The Dzhida Complex has been subdivided into three phases; the prevalent one is the early gabbro–granite association, represented by a complete set of rock compositions, from felsic to mafic. The syenites and monzonites of the second phase are also widespread, whereas the granites, leucogranites, and granosyenites of the third phase occur in a subordinate amount. Ore mineralization is limited to small molybdenum (Sokhatinskoe), molybdenum–tungsten (Buluktaevskoe), and base metal (Zun-Dabanskoe) deposits. In addition, gold placers and alluvial gold occurrences are widespread within the Buluktai–Kharatsai ore cluster (Gas'kov, 2019).

*Buluktaevskoe deposit.* The orefield of the Buluktaevskoe deposit is composed of the Paleozoic second-phase granosyenites and alaskite granites of the Gudzhir complex; spessartite, porphyry syenite and diorite, aplite, and porphyry granite dikes are also present (Buzkova, 1994) (Fig. 2). A specific feature of the deposit is its association with polymictic breccia, which forms a chimney-shaped body 107 × 120 m in size (Baturina and Ripp, 1984). The chimney dips northwestward at a steep angle (70°–75°). The host granosyenites are strongly greisenized over 80–110 m. Rock fragments in the breccia are composed of granitoids, dike, and metasedimentary rocks. The cement consists of a crushed and partially silicified and mineralized aggregate of the rocks listed above. In addition to the hydrothermal quartz, the cement contains fluorite, muscovite, calcite, and ore minerals (scheelite, pyrite, sphalerite, wolframite, etc.). Adjacent to the chimney is a ring-shaped breccia zone with stockwork-type mineralization, consisting of a network of multidirectional quartz–ore veinlets, molybdenite and hubnerite veins, and northwest-trending mafic and felsic dikes (Gordienko et al., 2018).

Three morphological types of ores have been recognized at the Buluktaevskoe deposit: stockwork ores, vein ores, and disseminated ores. The stockwork ores are spatially confined to the chimney-shaped body of brecciated rocks and repeat the chimney shape in plan view, having a concordant northwestward dip direction. The stockwork consists of molybdenite–wolframite–quartz veinlets with disseminated molybdenite mineralization in the greisenized wallrock granites. The overall dimensions of the stockwork body are 350 × 210 m. The average grades within the stockwork are 0.031% Mo and 0.162% $WO_3$. Vein ores are subordinate at the deposit. Veins occur both inside the stockwork and extend northwestward out of it. Mo grade ranges from a few hundredths to 0.1 wt % (average 0.025 wt %); $WO_3$ grade, from a few hundredths of to 6 wt % (average 0.2 wt %). Disseminated ores have a limited extent and occur in greisenized wallrock granitoids near quartz–molybdenite veins and veinlets. Separate zones of rich disseminated ores with Mo grades up to 6.12 wt % have been reported here.

Two mineralization stages have been established at the deposit, the early molybdenite and the late wolframite ones, separated by the intrusion of aplite dikes (Ripp, 1966; Kosals and Dmytrieva, 1973). The molybdenite stage includes three substages, the early epimagmatic molybdenite and the two hydrothermal molybdenite and quartz–molybdenite substages. The age of the ores is estimated at 144 ± 10 Ma (Savchenko et al., 2018). The wolframite stage includes the quartz–microcline, quartz–hubnerite–scheelite, and the late quartz–fluorite substages (Ripp, 1966).

## MATERIALS AND METHODS

In order to conduct research work, the results of which are presented in this article, ore samples were collected from the remaining surface mining workings at the Buluktaevskoe molybdenum–tungsten ore deposit. The greisenized granites with disseminated ore minerals (mostly molybdenite) and quartz veins and veinlets in the ore stockwork were sampled. Petrographic and metallographic descriptions were made under the Olympus BX-51 and Polar-3 metallographic microscopes. Analytical studies were carried out at the Geospectr Research Equipment Sharing Center (RESC) of the Dobretsov Geological Institute, Siberian Branch, Russian Academy of Science (GIN SB RAS), Ulan-Ude. The chemical composition of the minerals was determined at GIN SB RAS (Ulan-Ude) by X-ray spectral microanalysis under a LEO-1430VP scanning electron microscope with an INCA Energy 350 energy–dispersive spectrometer (analysts E.V. Khodyreva and S.V. Kanakin). The contents of U and Th in the ores were determined by X-ray phase analysis (XPA) (analysts B.Zh. Zhalsaraev, Zh.Sh. Rinchinova, and S.V. Bartanova). Rare earth element concentrations were determined by ICP-AES method (analyst I.V. Zvontsov).

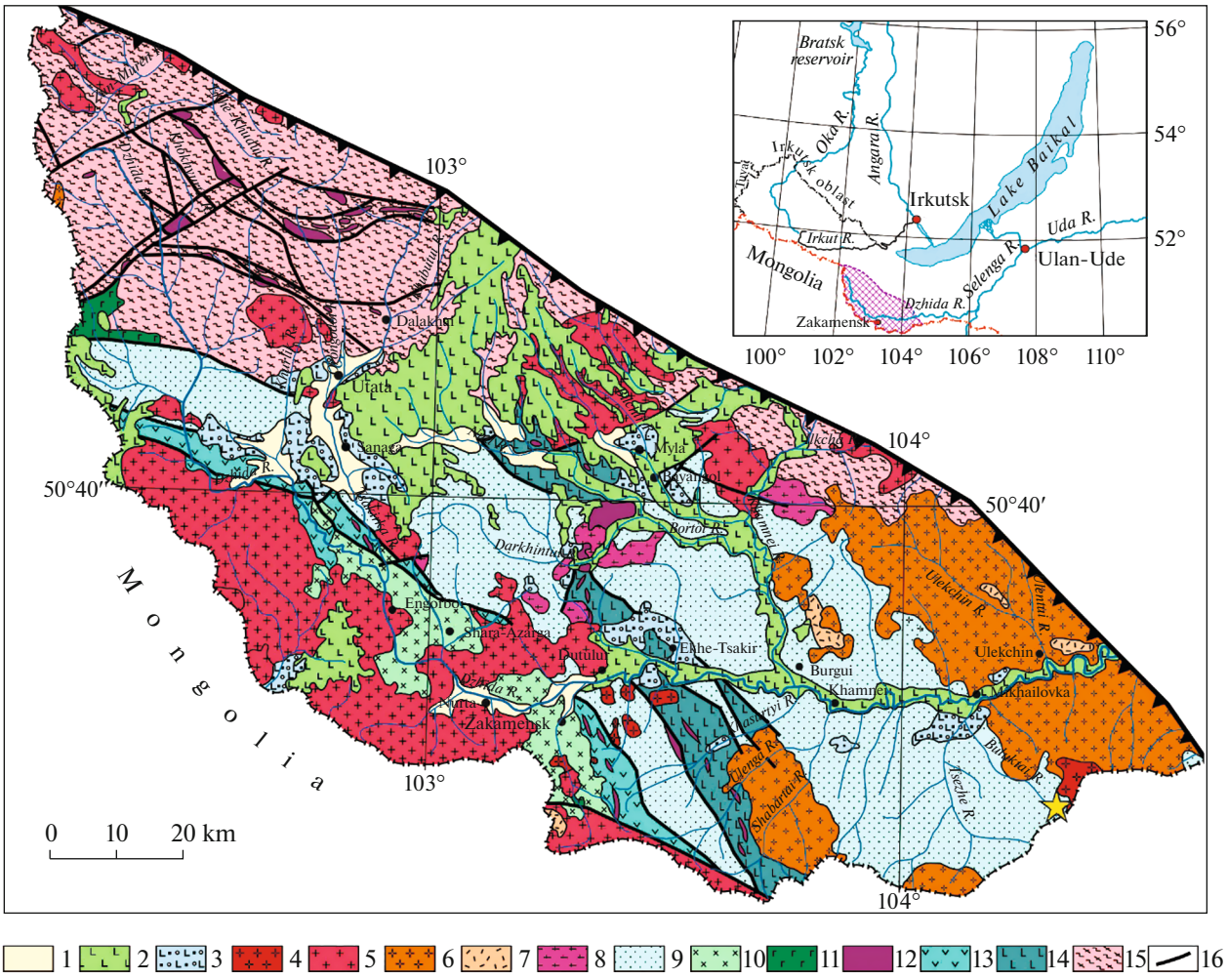


1 2 3 4 5 6 7 8 9 10 11 12 13 14 15 16

**Fig. 1.** Geological sketch map of Dzhida ore district (Gordienko et al., 2018). (1) Quaternary sediments; (2) Neogene–Quaternary basalts; (3) Jurassic–Cretaceous sedimentary and volcanosedimentary deposits; (4–7) intraplate (rift-related) complexes: (4) Mesozoic granitoids: Bichur ($P_2$-$T_1$), Malyi Kunalei ($T_{2-3}$), and Gudzhir ($J_3$-$K_1$) complexes; (5) Early Permian granitoids: Daban ($P_1$) and Shabartai ($P_1$) complexes; (6) Late Carboniferous granitoids: Bitu-Dzhida ($C_3$) and Ulekchin ($C_3$) complexes; (7) Permian–Carboniferous sedimentary–volcanic rocks (Gunzan Formation); (8) Cambrian–Ordovician early- and late-collisional granitoids (Late Dzhida Complex); (9) Cambrian–Ordovician sedimentary strata of back-arc and fore-arc paleobasins (Dzhida Formation); (10) Low–Middle Cambrian island-arc granitoids (Dzhida Complex); (11) Neoproterozoic island-arc gabbroids (Zungol complex); (12) Neoproterozoic basite–hyperbasites of ophiolite complex; (13) Neoproterozoic–Early Cambrian volcanic rocks of Dzhida island arc (Khokhyurta Formation); (14) Neoproterozoic–Early Cambrian sedimentary–volcanic rocks of Dzhidot seamount (guyot) (Khasurta Formation); (15) Neoproterozoic metasedimentary rocks of Khamardaban microcontinent (Khamardaban Group undifferentiated); (16) faults. Thick serrate line indicates northeastern boundary of Dzhida ore district. Asterisk indicates location of Buluktaevskoe deposit.

## MINERAL COMPOSITION OF MOLYBDENUM ORES

Gangue minerals of the quartz–molybdenite ores are represented predominantly by quartz; fluorite, muscovite, beryl, and carbonate (siderite) are present in smaller amounts (Fig. 3a). In addition, quartz, albite, potassium feldspar, biotite, and muscovite compose greisenized wallrock granites that contain molybdenite dissemination (Fig. 3b).

In addition to gangue minerals in the molybdenum ores, we identified 15 minerals, which, in addition to molybdenite, include sulfides (pyrite, galena, and chalcopyrite), tungstates (wolframite and scheelite), molybdates (powellite and wulfenite), and uranium–thorium–rare earth minerals, including the non-identified, probably new mineral species. Also, the ores contain accessory minerals: apatite, zircon, and rutile.

The main ore-forming mineral, **molybdenite**, forms radiolitic or platy aggregates, sometimes individual curved plates and intergrowths (Fig. 3c). It develops both in quartz veinlets and in the greisenized granitoid host rocks. Molybdenite is often associated with muscovite; the muscovite–molybdenite aggregates are sometimes characterized by joint growth structure,

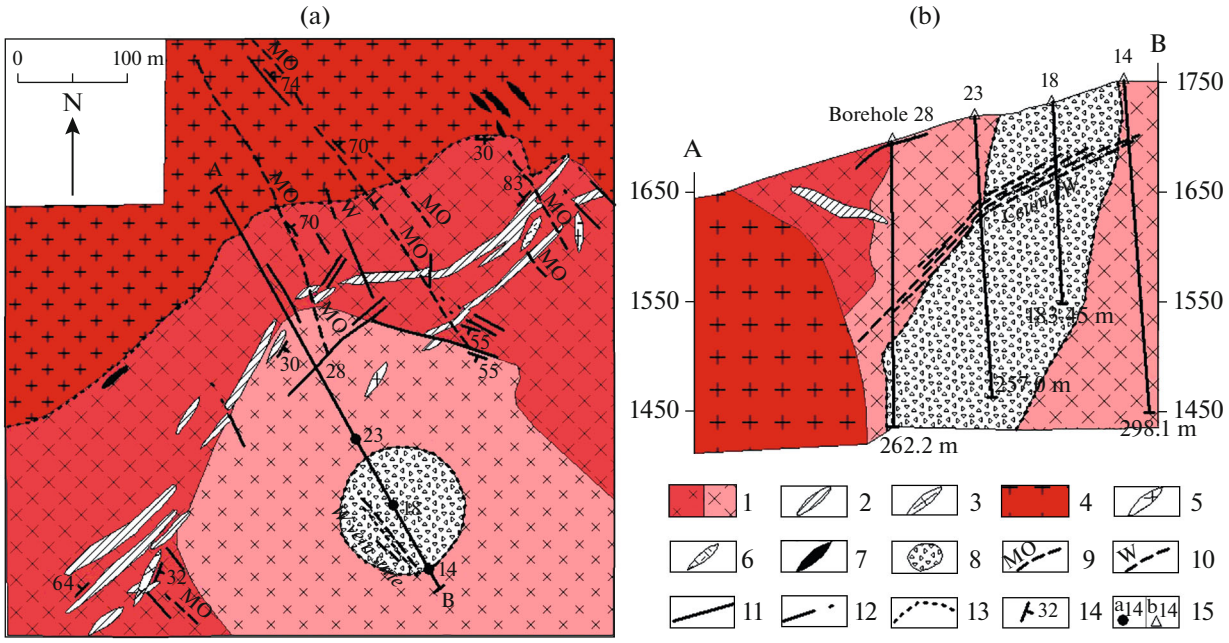


**Fig. 2.** Geological sketch map of Buluktaevskoe complex molybdenum–tungsten deposit (modified after Tugovik, 1974). (a) Map; (b) cross section along exploration profile A–B. (1) Upper Paleozoic quartz monzonite–syenites (a) and their brecciated varieties (b); (2–3) Upper Paleozoic dikes: (2) lamprophyres (odinite–spessartites); (3) porphyry diorites; (4) Early Mesozoic alaskite granites and alaskite granite dikes: (5) aplites; (6) porphyry granites; (7) ore-bearing explosive breccias; (8) polymict breccia of explosive chimney; (9–11) veins: (9) quartz–molybdenite, (10) quartz–hubnerite, (11) gangue quartz; (12) faults; (13) geological boundaries; (14) strike and dip symbols; (15) boreholes on map (a) and on cross section (b).

which indicates their nearly simultaneous formation. Molybdenite is also found in joint aggregates with potassium feldspar between quartz grains. In quartz veinlets, molybdenite develops both in the central parts of the veinlets and in selvages, sometimes in association with pyrite.

**Pyrite** is present in relatively small amounts as pockets or dissemination in granites and quartz–molybdenite veinlets and forms fractured aggregates of cubic grains. Molybdenite and rutile segregations are encountered in cracks in pyrite (Fig. 3d). As regards impurities in pyrite, Co in the amount of up to 0.66 wt % has been detected in single analyses, although in most cases pyrite does not contain impurities (within detection limits).

**Chalcopyrite** develops predominantly as scarce veinlets filling fractures in pyrite. In a single case it forms a drop-like segregation in quartz, in association with galena and wolframite.

**Galena** has been established only as microintergrowths with chalcopyrite and wolframite.

**Wolframite–hubnerite** ((Fe, Mn)$WO_4$) is associated with molybdenite (Fig. 3e). It forms subhedral roundish grains in quartz, sometimes as intergrowths with chalcopyrite and galena. The ores contain both minerals of wolframite–hubnerite series with similar FeO and MnO concentrations (11.02 and 12.80 wt %, respectively) and the mineral corresponding to hubnerite with FeO concentrations below 4.59 wt % (Table 1).

**Wulfenite** ($PbMoO_4$) is always associated with molybdenite and occurs as anhedral segregations in platy molybdenite aggregates, occasionally near molybdenite grains in quartz–chlorite aggregate (Fig. 3f). The mineral corresponds to its theoretical composition; impurities were not detected (see Table 1).

**Powellite** ($CaMoO_4$) is found as single grains in association with molybdenite, wulfenite, and monazite-(Ce) (Fig. 3g). Quartz and molybdenite are also present near powellite grains.

**Scheelite** ($CaWO_4$) is rarely found, predominantly in the mineralized greisenized granites, as microinclusions in rutile and fluorite (Figs. 3f, 3h)

Accessory minerals: apatite, zircon, monazite-(Ce), and rutile, often associated with U–Th minerals, were also found in the ores. However, monazite-(Ce) and rutile are found both in greisenized granites and in the quartz–molybdenite veinlets directly. The composition of monazite-(Ce), as a Th–REE-bearing mineral phase, is discussed in the next chapter.

**Rutile** forms crystals and angular crystal aggregates and is often heterogeneous due to the irregular distribution of impurities (Fig. 3h). A characteristic feature of rutile is the almost constant presence of Nb and V impurities in the amounts of 5.36 and 1.76 wt %, respectively (Table 2).

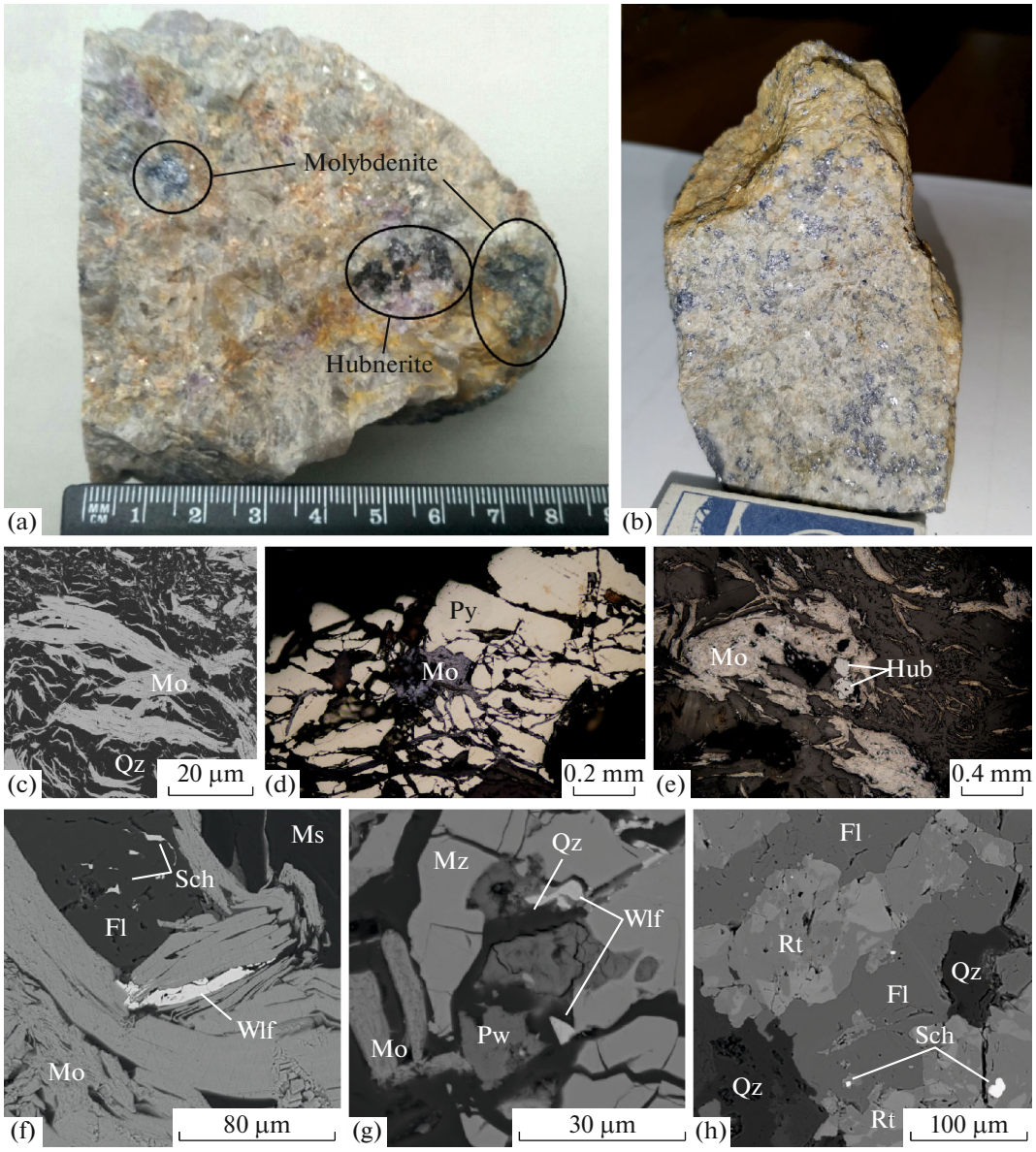


**Fig. 3.** Photographic images of samples and ore mineral morphology. (a) Photograph of a sample of molybdenite–hubnerite–quartz vein with fluorite; (b) photograph of a sample of disseminated molybdenite ore in greisenized granite; (c) morphology of molybdenite segregations (back-scattered electron image); (d) molybdenite that fills fractures in pyrite (reflected light image); (e) wolframite crystals in quartz–molybdenite aggregate; (f) anhedral wulfenite segregation in molybdenite aggregate; scheelite microinclusions in fluorite; (g) powellite crystal in association with wulfenite in a monazite-(Ce) grain; quartz fills cracks in monazite-(Ce); (h) heterogeneous rutile grains intergrown with fluorite and containing microinclusions of scheelite. Abbreviations of mineral names: Mo, molybdenite; Qz, quartz; Py, pyrite; Hub, wolframite (hubnerite); Wlf, wulfenite; Fl, fluorite; Ms, muscovite; Mz, monazite-(Ce); Pw, powellite; Rt, rutile.

**Zircon** occurs as subhedral roundish or rectangular grains, sometimes as euhedral prismatic crystals. Some grains were found to contain Hf impurity (1.36–2.41 wt %) (see Table 2).

**Apatite** occurs as single crystals, rectangular in cross section and up to 30 μm in size. X-ray spectral microanalysis of apatite showed the presence of up to 5.33 wt % F.

## REE, URANIUM, AND THORIUM MINERALS

A characteristic feature of the ores at the deposit is the wide spread and relatively large amount of U–Th–REE minerals. Such minerals as thorium-bearing monazite-(Ce), brannerite, thorite, uraninite, and the previously unknown and rare minerals, including fluorine-bearing thorium molybdate, orthobrannerite, and kobeite-(Y), were identified among them.

**Table 1.** Chemical compositions of molybdates and tungstates

| Seq | Sample index | FeO | MnO | MgO | CaO | $ThO_2$ | $MoO_3$ | $WO_3$ | PbO | $P_2O_5$ | Total |
|---|---|---|---|---|---|---|---|---|---|---|---|
| 1 | Bul_14 | 4.59 | 19.88 | | | | | 75.43 | | | 99.89 |
| 2 | Bul_14 | 4.02 | 18.95 | | | | | 76.43 | | | 99.40 |
| 3 | Bul_12 | 11.02 | 12.80 | | | | | 76.51 | | | 100.34 |
| 4 | Bul_18 | | | | | | 35. 83 | | 64. 65 | | 100.48 |
| 5 | Bul_18 | | | | | | 36.19 | | 63.55 | | 99.74 |
| 6 | Bul_23 | | | | | | 37.81 | | 60.89 | | 99.89 |
| 7 | Bul_18 | | | | | | 35.67 | | 64.20 | | 99.87 |
| 8 | Bul_23 | | | | | | 36.49 | | 63.03 | | 99.54 |
| 9 | Bul_18 | | | | | | 36.39 | | 62.93 | | 99.31 |
| 10 | Bul_18 | | | | | | 34.52 | | 65.79 | | 100.30 |
| 11 | Bul_23 | | | | | | 36.98 | | 63.16 | | 100.14 |
| 12 | Bul_23 | | | | | | 34.93 | | 65.09 | | 100.02 |
| 13 | Bul_6 | | | | | | 33.80 | | 66.05 | | 99.84 |
| 14 | Bul_6 | | | | | | 35.33 | | 64.35 | | 99.68 |
| 15 | Bul_23 | | | | 29. 20 | | 70.92 | | | | 100.12 |
| 16 | Bul_23 | 0.40 | | | 30.02 | | 68.68 | | | | 99.08 |
| 17 | Bul_23 | 1.58 | | | 20.78 | 6.48 | 64.76 | | 4.10 | 1.46 | 99.15 |
| 18 | Bul_18 | | | | 20.99 | | | 79.24 | | | 100.23 |
| 19 | Bul_18 | | | | 20.27 | | | 79.56 | | | 99.83 |

1–3, wolframite; 4–14, wulfenite; 15–17, powellite; 18–19, scheelite. Empty cell indicates concentration below detection limit.

The most common among the U–Th–REE minerals is **monazite-(Ce)**. It is confined predominantly to greisenized granites, but is also found in quartz–molybdenite veinlets. The mineral occurs as anhedral or subhedral isometric grains. It is often associated with rutile, apatite, and zircon and is sometimes replaced by fluorite (Fig. 4a) or molybdenite. In chemical composition, monazite-(Ce) is characterized by the prevalence of Ce and widely varying REE concentrations. $Ce_2O_3$ content in the mineral varies from 27.49 to 36.56 wt %; $La_2O_3$, from 12.89 to 23.98 wt % (Table 3). Also, the mineral contains 7.19–14.86 wt % $Nd_2O_3$, 1.50–3.71 wt % $Pr_2O_3$, and (in some grains) 1.32–2.01 wt % $Sm_2O_3$. Other REE concentrations are below detection limit. The concentrations of $ThO_2$ are widely varying from 1.43 to 14.86 wt %; moreover, high-Th monazite-(Ce) occurs as inclusions in the relatively low-Th variety (Fig. 4b). Sulfur impurity is noted in some analyzed grains, in which $SO_3$ content varies in the range of 0.68–1.2 wt %.

**Thorite** occurs as fine insets in fluorite and monazite-(Ce) (See Figs. 4a, 4b). The mineral contains rare earth elements, $Ce_2O_3$ (5.10–11.51 wt %), $La_2O_3$ (2.38–6.46 wt %), and $Nd_2O_3$ (2.04-4.06 wt %), as well as $P_2O_5$ (5.67–9.23 wt %) and CaO (0.52–1.38 wt %) (see Table 3). The concentrations of $UO_2$ are below the detection limit.

**Brannerite** was identified both in quartz veinlets and in the greisenized wallrock granites. The mineral forms anhedral microinclusions in rutile (Fig. 4c). The chemical composition of the mineral, according to X-ray spectral microanalysis data for two grains, is characterized by the presence of $Nb_2O_5$ (8.93–10.13 wt %), $Y_2O_3$ (4.05–4.53 wt %), and $ThO_2$ (3.04–3.28 wt %) (Table 4). In one case, iron impurity was established (1.04 wt % FeO).

A mineral that is similar in composition to brannerite (Fig. 4d), but differs from the latter by the shortage in total percentage (<100%), the presence of F as impurity (1.92–2.57 wt %), a relatively high $UO_2$ content (48.32–53.98 wt %), and a relatively low $TiO_2$ content (31.93–32.21 wt %) was also identified in association with muscovite and molybdenite (see Table 4). The deviation from 100% of the total percentage can be explained by the presence of the elements that cannot be determined in the mineral using electron probe microanalyzer (EPMA). Presumably, these are O and H, which can occur in the mineral as the OH hydroxyl group. In chemical composition this mineral corresponds to the hydroxyl-bearing uranium titanate, **orthobrannerite**, but the lack of X-ray data disables the reliable identification of this mineral. The calculation of $H_2O$ content in the mineral from the deficiency in the total percentage shows values of the order of 8.6–9.89 wt %. The empirical formula of the

**Table 2.** Chemical compositions of accessory minerals at Bulukaevskoe deposit

| Seq | Sample index | $SiO_2$ | $TiO_2$ | FeO | $V_2O_3$ | $ZrO_2$ | $HfO_2$ | $Nb_2O_5$ | Total |
|---|---|---|---|---|---|---|---|---|---|
| 1 | Bul 14 | | 98.78 | 1.00 | | | | | 99.76 |
| 2 | Bul 14 | | 99.24 | 0.53 | | | | | 99.76 |
| 3 | Bul 23 | 0.79 | 91.13 | 1.35 | 1.61 | | | 5.36 | 100.23 |
| 4 | Bul 14 | | 99.17 | 0.61 | 0.00 | | | | 99.78 |
| 5 | Bul 18 | | 95.12 | 1.66 | 0.66 | | | 2.15 | 99.59 |
| 6 | Bul 14 | | 96.09 | 2.65 | 0.80 | | | | 99.54 |
| 7 | Bul 23 | | 93.83 | 1.12 | 0.99 | | | 3.23 | 99.18 |
| 8 | Bul 12 | | 94.21 | 1.89 | 0.99 | | | 1.71 | 98.81 |
| 9 | Bul 21 | | 98.36 | 0.49 | 0.70 | | | 1.19 | 100.73 |
| 10 | Bul 14 | | 96.52 | 3.28 | | | | 0.84 | 100.65 |
| 11 | Bul 23 | | 94.78 | 0.92 | 1.34 | | | 3.58 | 100.63 |
| 12 | Bul 21 | | 97.65 | 0.74 | 0.70 | | | 1.03 | 100.11 |
| 13 | Bul 14 | | 94.83 | 3.58 | 0.00 | | | 1.70 | 100.10 |
| 14 | Bul 23 | | 93.76 | 1.13 | 1.43 | | | 3.29 | 99.60 |
| 15 | Bul 21 | | 94.54 | 0.52 | 1.76 | | | 2.72 | 99.54 |
| 16 | Bul 12 | | 96.47 | 1.29 | | | | 1.40 | 99.15 |
| 17 | Bul 12 | | 93.84 | 2.55 | | | | 4.15 | 100.54 |
| 18 | Bul 14 | | 94.01 | 3.82 | | | | 1.56 | 99.39 |
| 19 | Bul 18 | 32. 86 | | | | 67. 77 | 1.36 | | 101.99 |
| 20 | Bul 21 | 32.35 | | | | 67.66 | 1.42 | | 101.42 |
| 21 | Bul 6 | 32.86 | | | | 65.68 | 2.41 | | 100.94 |
| 22 | Bul 18 | 32.65 | | | | 67.19 | | | 99.84 |
| 23 | Bul 21 | 31.98 | | | | 65.85 | 1.9 | | 99.73 |
| 24 | Bul_21 | 30.96 | | | | 68.32 | | | 99.28 |

1–18, rutile; 19–24, zircon. Empty cell indicates concentration below detection limit.

mineral, calculated from X-ray spectral microanalysis data, corresponds to the theoretical formula ($U^{4+}U^{6+}Ti_4O_{12}(OH)_2$) and differs only by the presence of fluorine, which suggests isomorphism in OH–F series, characteristic of a series of uranium minerals (betafite, uranopyrochlore, etc.).

In addition to brannerite and orthobrannerite, the molybdenum ore contains one more Nb–Ti–U mineral with 7.78–19.46 wt % $Nb_2O_3$, 6.34–8.10 wt % $Y_2O_3$, and 3.22–4.80 wt % $ThO_2$, and also with a deficiency in the total percentage, which suggests the presence of the hydroxyl group in its formula (see Table 4). The calculation of $H_2O$ content from the deficiency in the total percentage shows values in the range of 8.0–13.81 wt %. The mineral is characterized by the presence of a large number of impurity components: $SiO_2$ (1.5–1.84 wt %), FeO (1.26–2.02 wt %), CaO (0.43–1.26 wt %), SrO (1.09–1.49 wt %), $Al_2O_3$ (0.53–0.85 wt %), and, in some grains, $Nd_2O_3$ (1.14–1.27 wt %). A mixed aggregate, consisting of the thin intergrowths of a niobium–titanium–uranium-bearing mineral aggregate, overgrows a rutile grain (Fig. 4e). In chemical composition the mineral, which constitutes this aggregate, corresponds to **kobeite-(Y)**, $(Y,U)(Ti,Nb)_2(O,OH)_6$, but is characterized by significant variations of major and impurity element concentrations. Nevertheless, in spite of a certain nonuniformity of the chemical composition, the calculation of the empirical formulas of the mineral demonstrates their similarity with the theoretical formula of kobeite-(Y), but the lack of X-ray data disables the reliable identification of this mineral.

**Uraninite** occurs as inclusions in rutile and quartz and as intergrowths with molybdenite and powellite, which gravitate toward the rutile segregations (see Fig. 4c). This mineral is characterized by the presence of $ThO_2$ (5.49–9.11 wt %) and PbO (1.16–1.33 wt %) as impurities (see Table 4). In one case, the impurities of $Y_2O_3$ (3.15 wt %) and FeO (0.99 wt %) are noted and U/O ratio is violated in the composition of uraninite, probably due to the epitaxial growth and $UO_2$ transformation into $UO_{2+x}$ (Dymkov, 1964).

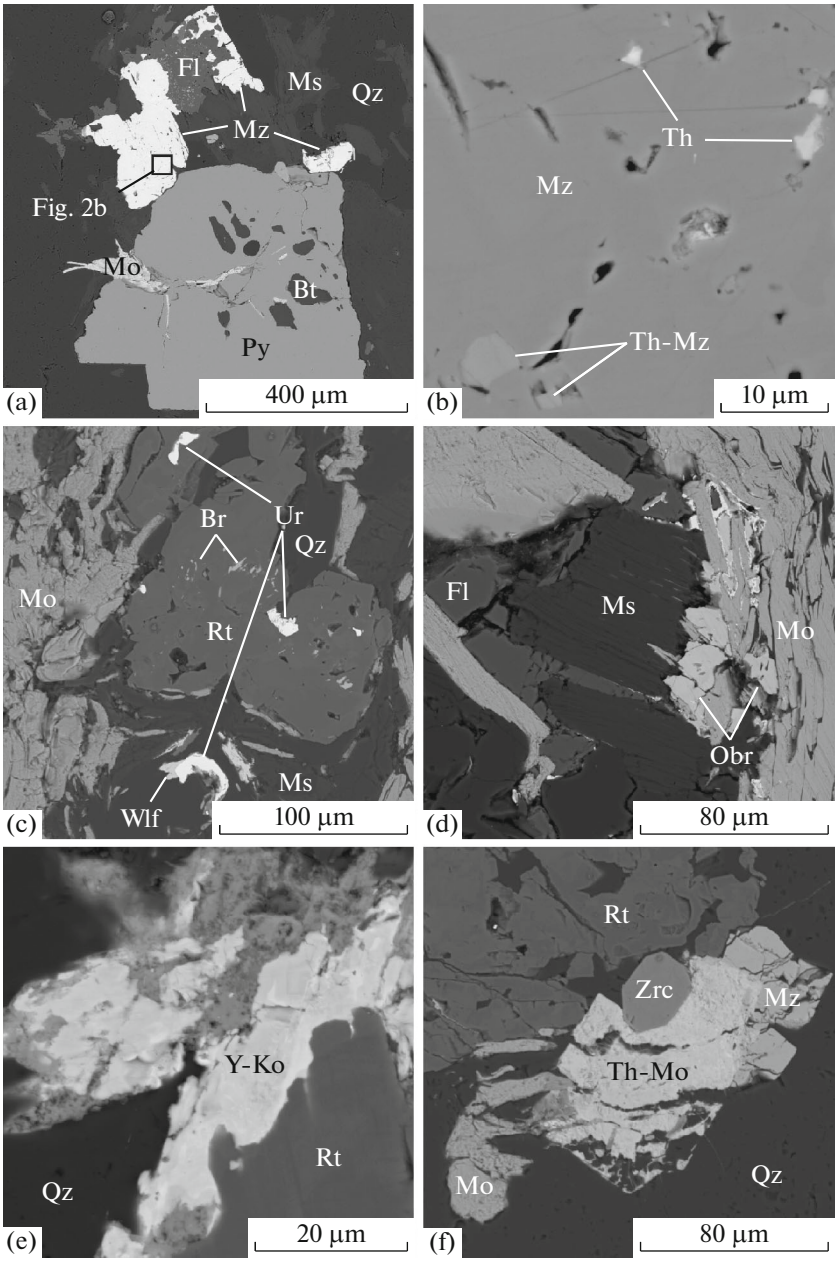


**Fig. 4.** Morphology of segregation of U–Th–REE-bearing minerals. (a) Monazite-(Ce) is replaced by fluorite that contains fine thorite dissemination; square shows location of Fig. 2b; (b) thorite microinclusions in monazite-(Ce); thorium-enriched segments of monazite-(Ce); (c) rutile grain, located near molybdenite aggregate, contains microinclusions of brannerite and uraninite grains; uraninite also forms intergrowth with wulfenite; (d) orthobrannerite grains in association with muscovite, fluorite, and molybdenite; (e) heterogeneous aggregate of kobeite-(Y), overgrowing rutile grain; gray aggregate corresponds to secondary Ti and Nb minerals containing U and Th impurities; (f) metacrystal (?) of thorium molybdate (Th-Mo) develops at boundary of rutile, molybdenite, and monazite grains (back-scattered electron images).

*Mineral name abbreviations:* Mo, molybdenite; Qz, quartz; Py, pyrite; Ms, muscovite; Fl, fluorite; Bt, biotite; Mz, monazite-(Ce); Th, thorite; Th-Mz, thorium-enriched monazite-(Ce); Rt, rutile; Wlf, wulfenite; Br, brannerite; Ur, uraninite; Obr, orthobrannerite; Y-Ko, kobeite-(Y); Th-Mo, thorium molybdate; Zrc, zircon.

In addition to the uranium–thorium–rare earth minerals, a previously unknown mineral species, **fluorine-bearing thorium molybdate**, was identified in a quartz–molybdenite veinlet. This mineral contains 49.66–55.43 wt % $ThO_2$ and 37.83–48.74 wt % $MoO_3$ (see Table 4). This mineral was encountered as a euhedral metacrystal that partially corrodes a monazite-(Ce) grain near rutile and zircon crystals. The metacrystal itself, in its turn, is partially replaced by molybdenite (Fig. 4f). X-ray spectral microanalysis of

**Table 3.** Chemical compositions and empirical formulas of monazite-(Ce) and thorite from ores of Buluktaevskoe deposit

| Seq | Sample index | $SiO_2$ | CaO | $Ce_2O_3$ | $La_2O_3$ | $Pr_2O_3$ | $Nd_2O_3$ | $Sm_2O_3$ | $ThO_2$ | $P_2O_5$ | $SO_3$ | Total |
|---|---|---|---|---|---|---|---|---|---|---|---|---|
| 1. | Bul_12 | | 0.74 | 30.52 | 21.29 | 1.50 | 7.48 | | 11.18 | 26.15 | 1.20 | 100.06 |
| 2. | Bul_12 | | | 30.80 | 21.61 | 3.31 | 7.19 | | 11.90 | 24.50 | 0.98 | 100.28 |
| 3. | Bul_23 | | 0.46 | 36.56 | 21.73 | 2.26 | 8.12 | | 1.62 | 30.06 | | 100.81 |
| 4. | Bul_18 | 0.79 | 0.39 | 35.00 | 23.98 | 1.60 | 7.33 | | 2.08 | 28.60 | | 99.77 |
| 5. | Bul_12 | | 0.55 | 35.19 | 21.70 | 1.97 | 8.78 | | 1.52 | 29.51 | | 99.21 |
| 6. | Bul_23 | | | 33.91 | 20.54 | 2.62 | 8.77 | 1.32 | 2.24 | 29.56 | | 98.96 |
| 7. | Bul_14 | | 1.10 | 32.58 | 12.89 | 3.71 | 14.09 | 2.01 | 2.39 | 30.78 | 0.68 | 100.25 |
| 8. | Bul_14 | | 1.53 | 32.66 | 12.97 | 3.60 | 14.86 | 1.96 | 1.36 | 31.15 | | 100.11 |
| 9. | Bul_14 | | 0.64 | 34.94 | 22.38 | 2.58 | 8.68 | | 1.54 | 28.70 | | 99.47 |
| 10. | Bul_21 | | 2.00 | 27.49 | 14.87 | 1.60 | 8.95 | | 14.86 | 29.41 | | 99.16 |
| 11. | Bul_12 | | 0.52 | 35.64 | 18.29 | 2.38 | 11.62 | | 1.43 | 30.16 | | 100.03 |
| 12. | Bul_12 | | 0.62 | 36.30 | 21.03 | | 8.64 | | 2.37 | 29.81 | 1.10 | 99.87 |
| 13. | Bul_12 | 15.51 | 1.38 | 5.10 | 2.38 | | 2.21 | | 67.90 | 5.67 | | 100.15 |
| 14. | Bul_12 | 13.73 | 0.95 | 11.51 | 6.46 | | 4.06 | | 54.24 | 9.23 | | 100.20 |
| 15. | Bul_12 | 14.49 | 0.52 | 8.80 | 4.31 | | 2.04 | | 62.08 | 7.21 | | 99.46 |

1. $(Ce_{0.481}La_{0.338}Nd_{0.115}Th_{0.110}Pr_{0.023}Ca_{0.034})_{\Sigma=1.102}(P_{0.954}S_{0.039})_{\Sigma=0.993}O_{3.905}$
2. $(Ce_{0.497}La_{0.351}Th_{0.119}Nd_{0.113}Pr_{0.053})_{\Sigma=1.134}(P_{0.914}S_{0.032})_{\Sigma=0.946}O_{3.920}$
3. $(Ce_{0.581}La_{0.348}Nd_{0.126}Pr_{0.036}Ca_{0.022}Th_{0.016})_{\Sigma=1.129}P_{1.104}O_{3.769}$
4. $(Ce_{0.542}La_{0.374}Nd_{0.110}Si_{0.034}Pr_{0.025}Th_{0.020}Ca_{0.018})_{\Sigma=1.122}P_{1.024}O_{3.854}$
5. $(Ce_{0.548}La_{0.340}Nd_{0.133}Pr_{0.031}Ca_{0.025}Th_{0.015})_{\Sigma=1.091}P_{1.063}O_{3.846}$
6. $(Ce_{0.566}La_{0.345}Nd_{0.143}Pr_{0.044}Th_{0.023}Sm_{0.021})_{\Sigma=1.142}P_{1.141}O_{3.718}$
7. $(Ce_{0.525}Nd_{0.221}La_{0.209}Pr_{0.059}Ca_{0.052}Sm_{0.031}Th_{0.024})_{1.121}(P_{1.147}S_{0.023})_{\Sigma=1.170}O_{3.709}$
8. $(Ce_{0.503}Nd_{0.223}La_{0.202}Ca_{0.069}Pr_{0.055}Sm_{0.028}Th_{0.013})_{\Sigma=1.094}P_{1.110}O_{3.796}$
9. $(Ce_{0.611}La_{0.395}Nd_{0.148}Pr_{0.045}Ca_{0.033}Th_{0.017})_{\Sigma=1.249}P_{1.162}O_{3.589}$
10. $(Ce_{0.429}La_{0.234}Th_{0.144}Nd_{0.136}Ca_{0.091}Pr_{0.025})_{\Sigma=1.059}P_{1.061}O_{3.880}$
11. $(Ce_{0.559}La_{0.289}Nd_{0.178}Pr_{0.037}Ca_{0.024}Th_{0.014})_{\Sigma=1.100}P_{1.093}O_{3.807}$
12. $(Ce_{0.555}La_{0.324}Nd_{0.129}Ca_{0.028}Th_{0.022})_{\Sigma=1.058}(P_{1.054}S_{0.035})_{\Sigma=1.089}O_{3.854}$
13. $(Th_{0.641}Ce_{0,077}Ca_{0.061}La_{0.037}Nd_{0.033})_{\Sigma=0.849}[(Si_{0.643}P_{0.199})_{\Sigma=0.842}O_{4.309}]$
14. $(Th_{0.565}Ce_{0,193}La_{0.109}Nd_{0.067}Ca_{0.047})_{\Sigma=0.981}[(Si_{0.628}P_{0.358})_{\Sigma=0.986}O_{4.035}]$
15. $(Th_{0.603}Ce_{0,137}La_{0.068}Nd_{0.031}Ca_{0.023})_{\Sigma=0.862}[(Si_{0.619}P_{0.26})_{\Sigma=0.879}O_{4.258}]$

1–12, monazite-(Ce); 13–15, thorite. Empty cell indicates concentration below detection limit.

the mineral in various points demonstrated a certain heterogeneity of this mineral, mostly due to the varying concentrations of both major elements (Th, Mo) and impurities: F (1.01–4.75 wt %), CaO (0.0–0.74 wt %), and $P_2O_5$ (0.0–2.08 wt %). In the absence of Ca and P impurities, the chemical composition of the mineral most completely corresponds to the formula $Th(MoO_4)_2$—double molybdate of thorium with F impurity.

To summarize, the molybdenum ores of the Buluktaevskoe deposit are characterized by relatively wide development of the U–Th–REE-bearing minerals, among which a previously unknown, probably new mineral species was identified.

The bulk U and Th concentrations in the ores, according to X-ray fluorescent analysis data, are relatively low, not higher than 28 and 32 ppm, respectively; in addition, the contents of these elements are widely varying (Table 5). The maximum uranium concentrations were established in quartz–molybdenite veinlets, whereas the relatively high thorium concentrations are more typical of the greisenized wallrock granites that contain disseminated molybdenite mineralization. At the same time, total REE concentrations are elevated and exceed 300 ppm in some samples (see Table 5). The most enriched in REE are the granites that contain disseminated molybdenite mineralization, but quartz–molybdenite veinlets also contain REE in concentrations up to 175 ppm.

**Table 4.** Chemical compositions and empirical formulas of U–Th minerals from ores of Buluktaevskoe deposit

| Seq | Sample index | $SiO_2$ | $TiO_2$ | $Al_2O_3$ | FeO | CaO | SrO | $Nd_2O_3$ | $Y_2O_3$ | $ThO_2$ | $UO_2$ | $MoO_3$ | PbO | $Nb_2O_5$ | $P_2O_5$ | F | Total |
|---|---|---|---|---|---|---|---|---|---|---|---|---|---|---|---|---|---|
| 1 | Bul_23 | | 41.26 | | | | | | 4.53 | 3.28 | 41.75 | | | 8.93 | | | 99.76 |
| 2 | Bul_23 | | 39.67 | | 1.04 | | | | 4.05 | 3.04 | 42.24 | | | 10.13 | | | 100.16 |
| 3 | Bul_6 | | 32.21 | | 0.82 | 2.04 | | | | 4.96 | 48.32 | | | | 0.48 | 2.57 | 91.4 |
| 4 | Bul_6 | | 31.93 | | 0 | 0.66 | | | | 1.63 | 53.98 | | | | | 1.92 | 90.11 |
| 5 | Bul_12 | 1.50 | 25.40 | 0.83 | 1.74 | 1.26 | 1.42 | 1.14 | 7.67 | 3.47 | 25.39 | | | 17.17 | | | 86.99 |
| 6 | Bul_12 | 1.69 | 25.09 | | 2.02 | 1.16 | 1.09 | 1.21 | 8.10 | 3.62 | 25.50 | | | 17.24 | | | 86.72 |
| 7 | Bul_12 | 1.20 | 26.59 | 0.85 | 1.75 | 0.66 | | 1.27 | 7.26 | 3.48 | 26.86 | | | 19.46 | | | 89.38 |
| 8 | Bul_12 | 1.73 | 32.24 | 0.53 | 1.69 | 0.43 | 1.61 | | 7.31 | 4.32 | 31.12 | | | 11.02 | | | 92.00 |
| 9 | Bul_12 | 1.84 | 31.53 | 0.70 | 1.88 | 0.66 | 1.49 | | 6.74 | 3.22 | 31.22 | | | 10.94 | | | 90.22 |
| 10 | Bul_12 | 1.73 | 29.42 | 0.60 | 1.39 | 0.56 | 1.36 | | 6.34 | 3.48 | 31.61 | | | 9.70 | | | 86.19 |
| 11 | Bul_12 | 1.56 | 35.45 | 0.64 | 1.26 | | 1.40 | | 6.62 | 4.80 | 32.37 | | | 7.78 | | | 91.87 |
| 12 | Bul_23 | | | | | | | | | 9.11 | 89.88 | | 1.16 | | | | 100.15 |
| 13 | Bul_23 | | | | | | | | | 8.00 | 89.86 | | 1.33 | | | | 99.18 |
| 14 | Bul_12 | | | | 0.99 | | | | 3.15 | 5.49 | 89.78 | | | | | | 99.41 |
| 15 | Bul_23 | | | | | 0.74 | | | | 55.43 | | 37.83 | | | 1.30 | 4.75 | 100.05 |
| 16 | Bul_23 | | | | | 0.64 | | | | 52.96 | | 41.57 | | | 2.08 | 2.20 | 99.46 |
| 17 | Bul_23 | | | | | 0.39 | | | | 49.61 | | 48.53 | | | | 1.18 | 99.70 |
| 18 | Bul_23 | | | | | 0.00 | | | | 49.66 | | 48.74 | | | | 1.01 | 99.41 |

1. $(U_{0.63}Th_{0.046}Y_{0.145})_{\Sigma=0.821}[(Ti_{1.998}Nb_{0.306}Fe_{0.058})_{\Sigma=2.362}O_{5.907}]$
2. $(U_{0.606}Th_{0.049}Y_{0.157})_{\Sigma=0.812}[(Ti_{2.026}Nb_{0.264})_{\Sigma=2.29}O_{5.988}]$
3. $(U_{1.98}Th_{0.06}Ca_{0.116})_{\Sigma=2.156}Ti_{3.958}O_{13.109}(OH_{1.000}F_{1.000})_{\Sigma=2}$
4. $(U_{1.762}Th_{0.184}Ca_{0.358})_{\Sigma=2.304}(Ti_{3.971}Fe_{0.113})_{\Sigma=4.084}O_{12.436}(OH_{0.669}F_{1.331})_{\Sigma=2}$
5. $(U_{0.352}Y_{0.254}Si_{0.094}Ca_{0.084}Al_{0.061}Th_{0.053}Sr_{0.051}Nd_{0.025})_{\Sigma=0.970}[Ti_{1.189}Nb_{0.483}Fe_{0.09}]_{\Sigma=1.762}(O,OH)_{6.268}$
6. $(U_{0.342}Y_{0.259}Si_{0.102}Ca_{0.075}Th_{0.050}Sr_{0.038}Nd_{0.026})_{\Sigma=0.891}[Ti_{1.136}Nb_{0.469}Fe_{0.102}]_{\Sigma=1.706}(O,OH)_{6.402}$
7. $(U_{0.389}Y_{0.252}Si_{0.078}Al_{0.065}Th_{0.051}Ca_{0.046}Nd_{0.030})_{\Sigma=0.911}[Ti_{1.301}Nb_{0.572}Fe_{0.095}]_{\Sigma=1.969}(O,OH)_{6.120}$
8. $(U_{0.440}Y_{0.248}Si_{0.110}Th_{0.063}Sr_{0.059}Al_{0.040}Ca_{0.030})_{\Sigma=0.989}[Ti_{1.543}Nb_{0.317}Fe_{0.090}]_{\Sigma=1.949}(O,OH)_{6.062}$
9. $(U_{0.423}Y_{0.219}Si_{0.113}Sr_{0.053}Al_{0.050}Th_{0.045}Ca_{0.043})_{\Sigma=0.946}[Ti_{1.445}Nb_{0.302}Fe_{0.095}]_{\Sigma=1.842}(O,OH)_{6.213}$
10. $(U_{0.470}Y_{0.225}Si_{0.116}Th_{0.053}Sr_{0.053}Al_{0.048}Ca_{0.04})_{\Sigma=1.004}[Ti_{1.478}Nb_{0.293}Fe_{0.077}]_{\Sigma=1.848}(O,OH)_{6.149}$
11. $(U_{0.455}Y_{0.222}Si_{0.099}Th_{0.069}Sr_{0.051}Al_{0.048})_{\Sigma=0.945}([Ti_{1.687}Nb_{0.222}Fe_{0.067}]_{\Sigma=1.976}(O,OH)_{6.080}$
12. $(U_{0.834}Th_{0.076}Pb_{0.015})_{\Sigma=0.925}O_{2.075}$
13. $(U_{0.821}Th_{0.085}Pb_{0.013})_{\Sigma=0.919}O_{2.081}$
14. $(U_{0.561}Y_{0.047}Th_{0.035}Fe_{0.023})_{\Sigma=0.666}O_{2.334}$
15. $(Th_{1.141}Ca_{0.071}P_{0.10})_{\Sigma=1.322}Mo_{1.429}O_{6.90}F_{1.482}$
16. $(Th_{1.023}Ca_{0.058}P_{0.15})_{\Sigma=1.231}Mo_{1.474}O_{7.704}F_{0.592}$
17. $(Th_{1.03}Ca_{0.058})_{\Sigma=1.088}Mo_{1.848}O_{7.745}F_{0.34}$
18. $Th_{1.032}Mo_{1.858}O_{7.819}F_{0.291}$

1–2, brannerite; 3–4, orthobrannerite(?), estimated $H_2O$ concentrations are 8.6–9.89 wt %; 5–11, kobeite-(Y)(?), estimated $H_2O$ concentrations are 8.0–13.81 wt %; 12–14, uraninite; 15–18, fluorine-bearing thorium molybdate. Empty cell indicates concentration below detection limit.

## RESULTS AND DISCUSSION

As a result of the studies, 15 ore-forming minerals represented by sulfides, tungstates, molybdates, and U–Th–REE minerals were identified in the molybdenum ores of the Buluktaevskoe deposit. Unlike other deposits of the Dzhida orefield, where wolframite is represented exclusively by hubnerite (Damdinova and Damdinov, 2021), in this case wolframite, containing Mn and Fe in comparable amounts, is also present along with hubnerite. Specific features of ores at the Buluktaevskoe deposit are elevated Nb and V concentrations in rutile. Nb impurities are characteristic of rutile from rare metal granites (Aurisicchio et al., 2002; Černý et al., 1999), whereas V is characteristic of rutile from the plutonic–hydrothermal gold deposits (Scott et al., 2011). The uranium–thorium–REE-bearing minerals are scarcely found in the ores of molybdenum–tungsten deposits directly: as a rule, they occur as single grains of accessory minerals, uraninite or brannerite (Borovikov et al., 2020; Moura

**Table 5.** U, Th, and total REE concentrations (ppm) in ores of Buluktaevskoe deposit

| Seq | Sample index | Rock type | Th | U | ΣREE |
|---|---|---|---|---|---|
| 1. | Bul 18 | Granite with molybdenite dissemination | | 14 | 317.6 |
| 2. | Bul 16 | Granite with molybdenite dissemination | | 10 | – |
| 3. | Bul 15 | Granite with molybdenite dissemination | | 31 | 89.5 |
| 4. | Bul 10 | Granite with quartz–beryl veinlet | 29 | 20 | 25.0 |
| 5. | Bul 19 | Granite with quartz–molybdenite veinlet | 4.5 | 11 | – |
| 6. | Bul 21 | Granite with quartz–molybdenite veinlet | 32 | 21 | – |
| 7. | Bul 22 | Quartz with sulfides | 2 | 14 | – |
| 8. | Bul 11 | Quartz with sulfides | 20 | 7.8 | 175.3 |
| 9. | Bul 12-1 | Quartz with sulfides | 18 | 7.4 | – |
| 10. | Bul 12-2 | Quartz with sulfides | 20 | 11 | – |
| 11. | Bul 6 | Quartz with sulfides | | 27 | 152.8 |
| 12. | Bul 7 | Quartz with sulfides | | 9.1 | 6.1 |
| 13. | Bul 2 | Quartz with fluorite and beryl | 13 | 13 | 77.1 |
| 14. | Bul 9 | Quartz–molybdenite veinlet | 6.7 | | 145.1 |
| 15. | Bul 9a | Quartz–molybdenite veinlet | 5.0 | 2.1 | – |
| 16. | Bul 13 | Pure molybdenite veinlet | | 28 | – |

Empty cell indicates concentration below detection limit; hyphen, not analyzed. Analyses of U and Th concentrations were carried out by XRF method, analyst B.Zh. Zhalsaraev; total REE concentrations, by ICP-AES method, analyst I.V. Zvontsov.

et al., 2014). Therefore, these minerals were not found in the ores of the Pervomaiskoe molybdenum deposit, the largest in the region, with the exception of single grains of monazite-(Ce) and uraninite (Damdinova et al., 2020).

The uranium–thorium–rare earth mineralization at the studied Buluktaevskoe molybdenum–tungsten deposit is represented by a number of minerals, some of which are extremely rare. Monazite-(Ce) as an accessory mineral is usually found in granitoids, but monazite-(Ce) grains and aggregates in the ores of the Buluktaevskoe deposit were also established in quartz–molybdenite veinlets, and this suggests the hydrothermal origin of at least some of them. This probably accounts for the variations of the chemical composition of monazite-(Ce), the widely different contents of Th, in particular. Considering that the studied granitoids are also undergone to hydrothermal metasomatic alteration, it is difficult to establish the origin of monazite-(Ce) in each particular case, because significant variations of the composition of this mineral are observed within a single sample. The solution of this problem requires more detailed studies of the accessory and hydrothermal monazite-(Ce). In this case, it was established that the Th-bearing monazite-(Ce) could be formed as a result of hydrothermal alteration together with other U–Th–REE minerals.

Brannerite is a fairly widespread mineral, known in the ores of hydrothermal and metamorphic uranium deposits as well as in complex gold–uranium deposits (Aleshin et al., 2007; Budyak et al., 2017; Mironov et al., 2008; Tarasov et al., 2018; Cuney et al., 2012; Steacy et al., 1974). However, orthobrannerite, distinguished by the presence of the hydroxyl group in its composition, is less widespread. Several known finds of this mineral in China, Italy, Mexico, and Slovakia are included in Mindat database (https://www.mindat.org/). Orthobrannerite finds in uranium ores at deposits in Aldan region were also described (Chernikov, 2012). The origin of this mineral is attributed to the weathering of uranium-bearing syenites, although it is also found in the hypogene hydrothermal U–Mo ores (Kohut et al., 2013). The mineral in the molybdenum ores of the Buluktaevskoe deposit, corresponding to orthobrannerite in composition, is obviously hypogene and is associated with molybdenite and muscovite. The presence of fluorine allows us to classify it preliminarily as an F-bearing orthobrannerite variety, but for a more accurate identification it is necessary to conduct additional studies and acquire X-ray data in the first instance.

The identified mineral, which composes the aggregate that overgrows the rutile segregation, is similar to kobeite in chemical composition. This mineral is extremely rare; its single finds were identified in pegmatites in Japan and New Zealand (Hutton, 1957; Masutomi et al., 1961; Takubo et al., 1950). The mineral that occurs in the ores of the Buluktaevskoe deposit has a heterogeneous chemical composition, but generally corresponds to the theoretical composition of kobeite-(Y), which is obvious from the empirical formulas of the mineral, calculated from X-ray spectral microanalysis data. The compositions of

kobeite, given in the cited sources, are characterized by certain features distinguishing it from the mineral identified in the studied ores, such as the presence of zirconium impurity and lower uranium content, but this mineral has been analyzed only by chemical analysis, which cannot detect the possible presence of the microinclusions of other minerals. At the same time, according to the theoretical formula of this mineral, it is non-stoichiometric; therefore, significant variations of the contents of the main elements are possible in the chemical composition of the mineral. As in the previous case, additional studies are required for more accurate identification.

Among the uncommon, previously unidentified minerals is the fluorine-bearing thorium molybdate. Unlike the newly identified mineral, the previously known thorium molybdates, ichnusaite ($Th(MoO_4)_2 \cdot 3H_2O$) and nuragheite ($Th(MoO_4)_2 \cdot H_2O$), are hydrous and do not contain fluorine (according to the mineralogical database at https://www.mindat.org/). These minerals were identified in a single location on Sardinia Island in Italy (Orlandi et al., 2015), where they were found in quartz veins of a Bi–Mo ore occurrence. The mineral that we identified is distinguished by the presence of fluorine and the absence of OH-group; in addition, fluorine content is varying. In spite of the small number of mineral identifications, it was noted that fluorine content is inversely related with Mo and directly correlates with Th (see Table 4). The crystalline structures of double thorium and alkali metal molybdates were studied by experiments (Bushuev and Trunov, 1975, etc.). The available data can also be applied to natural analogs, but it is necessary to conduct X-ray analysis of the studied mineral.

To summarize, judging by the morphology and interrelations between uranium–thorium minerals and the surrounding ore and rock-forming minerals, we may conclude that all of the studied U–Th–REE-bearing minerals formed as a result of hydrothermal processes. The association of these minerals with molybdenite and other ore minerals suggests their joint formation at the early (molybdenite) development stage of the Buluktaevskoe molybdenum–tungsten deposit and that these minerals were not found in the ores of the later wolframite stage.

The origin of the U–Th–REE-bearing minerals can be due to the effect of the rare–metal Li–F granites, which are among the established sources of uranium (Aleshin et al., 2007). The effect of rare-metal magmatism indirectly confirms the presence of Nb impurity in the accessory rutile. However, Li–F granites were not established in the orefield of the Buluktaevskoe deposit, although such granites are known in the Dzhida ore district (Antipin and Perepelov, 2011).

## CONCLUSIONS

1. Fifteen ore-forming minerals were established in the molybdenum ores of the Buluktaevskoe deposit, including, in addition to molybdenite, sulfides (pyrite, galena, and chalcopyrite); tungstates (wolframite and scheelite); molybdates (powellite and wulfenite); and U–Th–REE-bearing minerals.

2. A characteristic feature of the ores of this deposit is the wide development and relatively large number of the mineral species of U–Th–REE minerals. Among them are monazite-(Ce); brannerite; thorite; uraninite; a previously unknown mineral species: fluorine-bearing thorium molybdate; and minerals similar in composition to orthobrannerite and kobeite-(Y).

3. All of the studied uranium–thorium–rare earth minerals formed during hydrothermal process at the early (molybdenite) development stage of the Buluktaevskoe molybdenum–tungsten deposit.

## ACKNOWLEDGMENTS

The authors are grateful to the anonymous reviewers for careful reading of the manuscript and comments, which enabled us to improve it.

## FUNDING

The study was supported by the Ministry of Science and Higher Education of the Russian Federation (state task for the Geological Institute, Siberian Branch, Russian Academy of Sciences, topic no. AAAA-A21-121011390003-9).

## CONFLICT OF INTEREST

The author declares that he has no conflict of interest.



## REFERENCES

Aleshin, A.P., Velichkin, V.I., and Krylova, T.L., Genesis and formation conditions of deposits in the unique Strel'tsovka molybdenum–uranium ore field: new mineralogical, geochemical, and physicochemical evidence, *Geol. Ore Deposits,* 2007, vol. 49, no. 5, pp. 392–412.

Antipin, V.S. and Perepelov, A.B., Late Paleozoic rare-metal granitoid magmatism of the southern Baikal Region, *Petrology,* 2011, vol. 19, no. 4, pp. 370–381.

Aurisicchio, C., De Vito, C., Ferrini, V., and Orlandi, P., Nb and Ta oxide minerals in the Fonte del Prete granitic pegmatite dike, Island of Elba, Italy, *Can. Mineral.,* 2002, vol. 40, pp. 799–814.

Baturina, E.E. and Ripp, G.S., *Molibdenovye i vol'framovye mestorozhdeniya Zapadnogo Zabaikal'ya* (Molybdenum and Tungsten Deposits of Western Transbaikalia), Moscow: Nauka, 1984.

Borovikov, A. A., Gushchina, L. V., Goverdovskii, V. A., and Gimon, V. O. Physicochemical conditions of ore formation at the Kalguty Mo–W deposit: thermodynamic modeling, *Geochem. Int.,* 2020, vol. 58, no. 1, pp. 27–39.

Bortnikov, N.S., Volkov, A.V., Galyamov, A.L., Vikent'ev, I.V., Aristov, V.V., Lalomov, A.V., and Murashov, K.Yu., Mineral resources of high-tech metals in Russia: state of the art and outlook, *Geol. Ore Deposits,* 2016, vol. 58, no. 2, pp. 83–103.

Budyak, A.E., Parshin, A.V., Spiridonov, A.M., Reutskii, V.N., Damdinov, B.B., Volkova, M.G., Tarasova, Yu.I., Abramova, V.A., Bryukhanova, N.N., and Zarubina, O.V., Geochemical controls on the formation of unconformity-type Au–U deposits (Northern Transbaikalia), *Geochem. Int.,* 2017, vol. 55, no. 2, pp. 184–194.

Bushuev, N.N. and Trunov, V.K., Double molybdates of rubidium and thorium, *Zh. Neorg. Khimii,* 1975, vol. 20, no. 4, pp. 1143–1144.

Buzkova, N.G., New data on relations of granitoid magmatism with endogenous mineralization: evidence from the Buluktai massif in Western Transbaikalia, *Dokl. Akad. Nauk,* 1994, vol. 338, no. 6, pp. 793–797.

Černý, P., Chapman, R., Simmons, W.B., and Chackowsky, L.E., Niobian rutile from the McGuire granitic pegmatite, Park County, Colorado: solid solution, exsolution, and oxidation, *Am. Mineral.,* 1999, vol. 84, pp. 754–763.

Chernikov, A.A., Complex uranium oxides in uranium ores, *New Data on Minerals,* 2012, vol. 47, pp. 71–83.

Cuney, M., Emertz, A., Mercadier, J., Mykchaylov, V., Shunko, V., and Yuslenko, A., Uranium deposits associated with Na-metasomatism from Central Ukraine: a review of some of the major deposits and genetic constraints, *Ore Geol. Rev.,* 2012, vol. 44, pp. 82–106.

Damdinova, L.B., Damdinov, B.B., Huang, X.-W., Bryansky, N.V., Khubanov, V.B., and Yudin, D.S., Age, conditions of formation, and fluid composition of the Pervomaiskoe molybdenum deposit (Dzhidinskoe ore field, South-Western Transbaikalia, Russia), *Minerals,* 2019, vol. 9, p. 572.

Damdinova, L.B. and Damdinov, B.B., Tungsten ores of the Dzhida W–Mo ore field (Southwestern Transbaikalia, Russia): mineral composition and physical-chemical conditions of formation, *Minerals,* 2021, vol. 11, p. 725.

Dymkov, Yu.M., Epitaxial transformations $U_3O_8 > UO_{2+x}$ in pitchblend, *Dokl. Akad. Nauk SSSR,* 1964, vol. 157, no. 3, pp. 583–585.

Gas'kov, I.V., Hydrothermal zones as possible sources of placer gold of the Buluktai–Kharatsai ore cluster (Dzhida ore cluster of Buryatia), *Geol. Mineral.-Syr'ev. Res. Sibiri,* 2019, no. 2, pp. 82–92.

Gordienko, I.V., Gorokhovskii, D.V., Smirnova, O.K., Lantseva, V.S., Badmatsyrenova, R.A., and Orsoev, D.A., Dzhida ore district: geology, structural, and metallogenic regionalization, genetic types of ore deposits, geodynamic conditions of their formation, forecast, and outlook for development, *Geol. Ore Deposits,* 2018, vol. 60, no. 1, pp. 1–32.

Hutton, C.O., Kobeite from Paringa River, south Westland, New Zealand, *Am. Mineral.,* 1957, vol. 42, pp. 342–353.

Kiseleva, G.D., Laputina, I.P., Chukhrova, O.F., and Tyuleneva, V.M., U–Th and Au–Bi–Te–Zn mineralization of the unique rare metal-tin deposit Syrymbet (Republic of Kazakhstan), *16th General Meet. IMA. Abstr.,* Piza (Italy): 1994, pp. 205– 206.

Kohut, M., Trubac, J., Novotny, L., Ackerman, L., Demko, R., Bartalsky, B., and Erban, V., Geology and Re–Os molybdenite geochronology of the Kuriškova U–Mo deposit (western Carpathians, Slovakia), *J. Geosci.,* 2013, vol. 58, pp. 275–286.

Kosals, Ya.A. and Dmitriyeva, A.N., Sequences and temperatures in formation of the Buluktay molybdenum–tungsten deposit (southwestern Transbaykal), *Int. Geol. Rev.,* 1973, vol. 15, no. 1, pp. 25–30.

Masutomi, K. and Nagashima, Kato A., Kobeite from the Ushio Mine, Kyoto prefecture, Japan, and re-examination of kobeite, *Mineral. J. (Japan),* 1961, vol. 3, pp. 139–147.

Mironov, A.G., Karmanov, N.S., Mironov, A.A., and Khodyreva, E.V., Gold–brannerite nuggets in placers of the Ozernoe ore cluster, *Russ. Geol. Geophys.,* 2008, vol. 49, no. 10, pp. 743–748.

Moura, A., Dória, A., Neiva, A.M.R., Leal, GomesC., and Creaser, R.A., Metallogenesis at the Carris W–Mo–Sn deposit (Gerês, Portugal): Constraints from fluid inclusions, mineral geochemistry, Re-Os and He-Ar isotopes," *Ore Geol. Rev.,* 2014, vol. 56, pp. 73–93.

Orlandi, P., Biagioni, C., Bindi, L., and Merlino, S., Nuragheite, $Th(MoO_4)\cdot 2H_2O$, the second natural thorium molybdate and its relationships with ichnusaite and synthetic $Th(MoO_4)_2$, *Am. Mineral.,* 2015, vol. 100, pp. 267–273.

Rekharskii, V.I., *Geokhimiya molibdena v endogennykh protsessakh* (Geochemistry of Molybdenum in Endogenous Processes), Moscow: Nauka, 1973.

Ripp, G.S., New data on the stage formation of the Buluktaev molybdenum–tungsten deposit, *Mater. po geologii i poleznym iskopaemym Buryatskoi ASSR,* 1966, vol. 10, pp. 155–168.

Ripp, G.S, Smirnova, O.K, Izbrodin, I.A., Lastochkin, E.I., Rampilov, M.O., and Posokhov, V.F., An isotope study of the Dzhida Mo–W ore field (Western Transbaikalia, Russia), *Minerals,* 2018, vol. 8, p. 546.

Rundqvist, D.V., Denisenko, V.K., and Pavlova, I.G., *Greizenovye mestorozhdeniya: ontogenez i filogenez* (Greisen Deposits: Ontogenesis and Phylogenesis), Moscow: Nedra, 1971.

Scott, K.M., Radford, N.W., Hough, R.M., and Reddy, S.M., Rutile compositions in the Kalgoorlie goldfields and their implications for exploration, *Austral. J. Earth Sci.: Int. Geosci. J. Geol. Soc. Austral.,* 2011, vol. 58, no. 7, pp. 803–812.

Steacy, H.R., Plant, R., and Boyle, R.W., Brannerite associated with native gold at the Richardson mine, Ontario, *Can. Mineral.,* 1974, vol. 12, pp. 360–363.

Takubo, J., Ukai, Y., and Minato, T., Studies on the minerals containing rare elements (Part II). A new mineral found in Kobe-Mura, Kyoto prefecture, Japan, *Chishitsugaku Zasshi,* 1950, vol. 56, pp. 509–513.

Tarasov N.N., Kochkin B.T., Velichkin V.I., and Doinikova O.A. Deposits of the Hiagda uranium ore field, Buryatia: formation conditions and ore control factors, *Geol. Ore Deposits,* 2018, vol. 60, no. 4, pp. 347–354.

Tugovik, G.I., *Eksplozii i rudnyi protsess* (Explosions and Ore Processes), Moscow: Nedra, 1974.

*Translated by E. Murashova*